100 YEARS Journal of Ecology

British Ecological Society

Journal of Ecology doi: 10.1111/1365-2745.12497

Variation and macroevolution in leaf functional traits in the Hawaiian silversword alliance (Asteraceae)

Benjamin Blonder[1,2]*, Bruce G. Baldwin[3], Brian J. Enquist[2,4] and Robert H. Robichaux[2,5]

[1]Environmental Change Institute, School of Geography and the Environment, University of Oxford, South Parks Road, Oxford OX1 3QY, UK; [2]Department of Ecology and Evolutionary Biology, University of Arizona, 1041 E Lowell St., Tucson, AZ 85721, USA; [3]Jepson Herbarium and Department of Integrative Biology, University of California, 1001 Valley Life Sciences Building 2645, Berkeley, CA 94720, USA; [4]The Santa Fe Institute, 1399 Hyde Park Road, Santa Fe, NM 87501, USA; and [5]Hawaiian Silversword Foundation, PO Box 1097, Volcano, HI 96785, USA

Summary

1. The Hawaiian silversword alliance is a spectacular example of plant adaptive radiation. The lineage includes 33 species in three endemic genera (*Argyroxiphium*, *Dubautia* and *Wilkesia*) that occupy almost all major habitats of the Hawaiian archipelago.

2. Here, we quantitatively explore functional diversification in the lineage by linking measurements of multiple leaf functional traits with climate niche and phylogenetic data.

3. We show that leaf functional trait variation (i) spans much of the global angiosperm range, (ii) is best explained by a white-noise evolutionary model and (iii) is integrated in ways consistent with both the global leaf economics spectrum and the predictions of leaf venation network theory.

4. Our results highlight the importance of functional diversification and integration in rapidly evolving plant lineages. They also provide compelling additional support for the view that the Hawaiian silversword alliance is one of the world's premier examples of adaptive radiation in plants.

Key-words: adaptive radiation, climate niche, ecophysiology, functional trait, silversword alliance, vein density, vein elongation index, venation network

Introduction

The Hawaiian silversword alliance (Asteraceae) is 'one of the most remarkable examples of adaptive radiation in plants' (Raven, Evert & Eichhorn 2013) because of the major ecological changes that have accompanied its unusually rapid diversification (Baldwin 2003). The lineage includes 33 species in three endemic genera (*Argyroxiphium*, *Dubautia* and *Wilkesia*) that evolved from a single colonizing ancestor arriving from western North America ca. 4–6 Mya (Baldwin & Sanderson 1998; Barrier *et al.* 1999). Species occur on all six of the main Hawaiian islands (Carr 1985). The lineage has diversified across habitats as varied as exposed lava, dry shrubland, dry woodland, mesic forest, wet forest and bog, with the species ranging in elevation from < 100 m to > 3700 m (Carr 1985; Robichaux *et al.* 1990). The lineage also includes a broad diversity of growth habits, such as rosette shrubs, shrubs, trees and lianas, and of leaf forms and venation patterns (Fig. 1).

To provide a more quantitative understanding of this diversity, we examine variation in leaf functional traits and macroevolutionary patterns of trait–trait and trait–climate relationships for 32 silversword alliance taxa. Specifically, we (i) assess variation in leaf functional traits across the silversword alliance in relation to the global angiosperm range, (ii) analyse the trait–trait and trait–climate relationships in the context of contrasting macroevolutionary models and (iii) determine whether the leaf functional trait variation is integrated (strongly inter-correlated) in ways consistent with both the global leaf economics spectrum and the predictions of physiological theory.

Current patterns of trait–trait and trait–climate relationships may be explained by contrasting macroevolutionary models that may underlie lineage diversification (Wiens *et al.* 2010; Crisp & Cook 2012; Pyron *et al.* 2015). On the one hand, the evolution of new trait values may be constrained by phylogenetic niche conservatism, defined as the retention of niche-related ecological traits over time among related taxa (Wiens, 2004; Wiens *et al.* 2010). This scenario is most consistent with either a random-walk evolutionary model (Brownian correlation structure) or an Ornstein–Uhlenbeck (frictional random-walk) evolutionary model (Martins correlation structure) (Wiens *et al.* 2010; Crisp & Cook 2012; Pyron *et al.* 2015). Among the suite of factors that may contribute

*Correspondence author: E-mail: bblonder@gmail.com

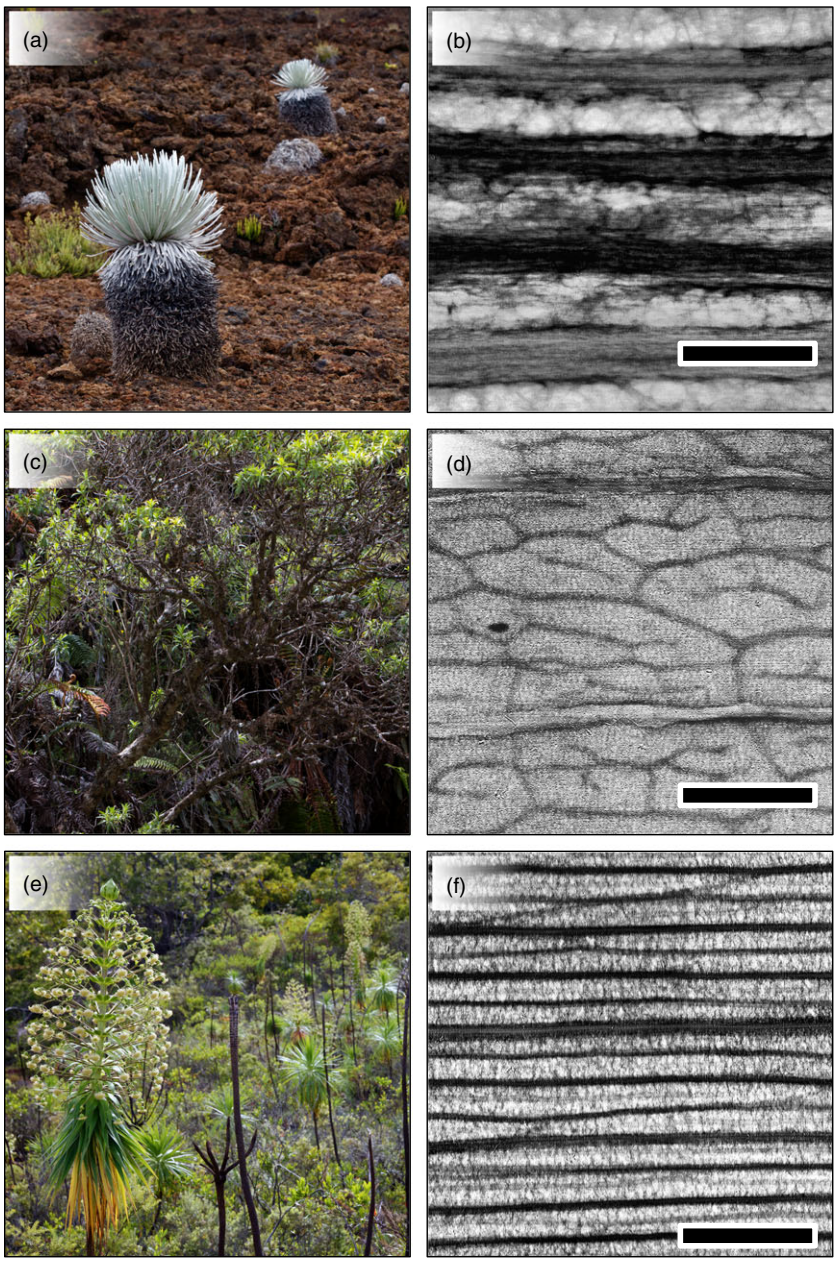

Fig. 1. Examples of habitat, growth habit and leaf functional trait diversification in the silversword alliance. (a) *Argyroxiphium sandwicense* subsp. *sandwicense* inhabits dry subalpine shrublands on Mauna Kea (Hawai'i). It grows in rosette shrub form with lanceolate to linear leaves and (b) has highly parallel leaf venation network geometry of low density (VD = 1.6 mm^{-1}, VEI $\geq$ 10.5). (c) *Dubautia reticulata* inhabits mesic to wet forests on Haleakalā (Maui). It grows in tree form with lance-elliptic leaves and (d) has highly reticulate leaf venation network geometry of high density (VD = 4.3 mm^{-1}, VEI $\geq$ 4.0). (e) *Wilkesia gymnoxiphium* inhabits dry shrublands on Kaua′i. It grows in rosette shrub form with linear leaves and (f) has semi-reticulate leaf venation network geometry of high density (VD = 6.7 mm^{-1}, VEI $\geq$ 21.6). Scale bar for panels b, d and f is 1 mm.

to phylogenetic niche conservatism are stabilizing selection and the impeding effects of gene flow on trait evolution. On the other hand, the evolution of new trait values may be unconstrained by phylogeny, such that niche-related ecological traits are not retained over time among related taxa. This scenario is most consistent with a white-noise evolutionary model (no phylogenetic correlation structure) (Wiens *et al.* 2010; Crisp & Cook 2012; Pyron *et al.* 2015). Distinguishing among these contrasting macroevolutionary models may provide key insight into the magnitude of historical constraints on functional trait variation and integration during lineage diversification.

For plants, leaf hydraulics may play an important role in structuring trait–trait and trait–climate relationships (Sack & Holbrook 2006; Brodribb, Feild & Jordan 2007; Brodribb, Feild & Sack 2010). In particular, leaf venation network traits are important in water transport, sugar transport, mechanical support and damage resistance (Brodribb, Feild & Jordan 2007; Blonder *et al.* 2011; Sack & Scoffoni 2013). These traits vary widely across lineages (Ellis *et al.* 2009), with strong shifts occurring contemporaneously with the diversification of the angiosperms (Boyce *et al.* 2009).

Recent theory (Blonder *et al.* 2011; Blonder, Violle & Enquist 2013) suggests that leaf venation networks may mediate the integration of leaf functional traits evident in the global leaf economics spectrum (Wright *et al.* 2004) and may be linked to variation in climate (Blonder & Enquist 2014). We summarize these hypotheses in the following paragraphs, noting that they are all shown together in the path diagram proposed in Fig. 4 and then evaluated in the Results.

The theory is based on the assumption that selection has optimized leaf hydraulics via leaf venation network traits and

a set of traits associated with leaf conductance and allocation. The geometry of venation networks imposes structural constraints on leaf architecture and allocation. In this theory, higher minor vein density in leaves [VD; mm vein/mm^2 leaf area (Brodribb, Feild & Jordan 2007)] should be associated with higher leaf nitrogen concentration (N_m; %) and thus higher photosynthetic capacity, because higher VD enables a higher transpiration rate, which in turn allows a higher carbon uptake rate. Additionally, optimization of water transport per cost implies that leaf thickness should be proportional to inter-vein distance (the inverse of VD) (Noblin *et al.* 2008). Thus, higher VD is predicted to be associated with lower leaf thickness (*d*; mm) and lower leaf mass per unit area (LMA; g m^{-2}), although in sunlit vs. shaded environments the relationships can be reversed (Blonder, Violle & Enquist 2013). Tests of this theory have been positive across species (Blonder *et al.* 2014) and among genotypes of *Populus tremuloides* (Blonder, Violle & Enquist 2013) and *Arabidopsis thaliana* (Blonder *et al.* 2015). Nonetheless, this theory has been criticized for being overly simplistic in its modelling of water transport and carbon allocation, as well as for its limited empirical support (Sack *et al.* 2013; Li *et al.* 2015). In response, the theory's original authors have asserted that the theory does provide a useful baseline for incorporating more biological detail and offers a reasonable compromise between realism and generality (Blonder *et al.* 2014).

Specific mechanisms also may link variation in leaf venation networks to variation in climate. A key conjecture is that plant water supply should be coupled to environmental water supply (Blonder & Enquist 2014) via coordination of veins and stomata (Brodribb, Jordan & Carpenter 2013). Based on a proportional relationship between maximum leaf evapotranspiration rate and maximum site actual evapotranspiration, this theory predicts that higher VD should be associated with higher temperatures (measured here as minimum annual temperature; T_{min}, °C) and aridity (measured here as the ratio of mean annual precipitation to mean annual potential evapotranspiration; AI, dimensionless). Such correlations have previously been found in broad meta-analyses and within some clades along environmental gradients (reviewed in Sack & Scoffoni 2013).

In addition to their density, leaf venation networks are characterized by their reticulation. Reticulation is thought to be adaptive in some contexts. Multiple hypotheses have focused on hydraulic efficiency vs. redundancy trade-offs (Stamatakis, Hoover & Roguemont 2008; Katifori, Szöllősi & Magnasco 2010; McKown, Cochard & Sack 2010). Specifically, reticulation is thought to be more common in less hydraulically demanding and more shaded environments (Givnish *et al.* 2005; Sack & Scoffoni 2013). A more reticulate network has a higher carbon cost in terms of increased VD to supply or support the same area as a more parallel network (Price & Weitz 2014), but with the potential benefit of a higher number of redundant flow pathways in case of damage (Katifori, Szöllősi & Magnasco 2010; McKown, Cochard & Sack 2010). Here we measure reticulation with an elongation index (VEI; dimensionless) that reflects the ratio of the long axis to the short axis of each areole. An areole is defined as a region of lamina enclosed by a loop of veins that encloses no smaller loops (Ellis *et al.* 2009). For VEI $\approx$ 1, network geometry is maximally reticulate. For VEI >> 1, network geometry is highly parallel. Unlike a previously proposed loopiness metric (number of areoles per unit leaf area) (Blonder *et al.* 2011), VEI is scale independent and thus is more useful for representing an orthogonal axis to the scale-dependent VD.

Other traits not directly linked to leaf venation networks may further modulate functional integration. Leaf area (LA, cm^2) may influence leaf economics because of nonlinear scaling of mechanical support costs (Niinemets *et al.* 2007). Additionally, leaf carbon content (C_m; %), phosphorus content (P_m; %), $\delta^{13}C$ (per mil) and $\delta^{15}N$ (per mil) may have important stoichiometric roles within the leaf economics spectrum (Wright *et al.* 2004). Finally, leaf elongation ratio (length divided by maximum width; LER, dimensionless) may influence leaf energy balance (Nicotra *et al.* 2011) and thus leaf economics, as may leaf pubescence and growth habit.

Materials and methods

COLLECTIONS

We measured leaf functional traits (Table 1) for 32 silversword alliance taxa (29 species, plus several subspecies), comprising a total of 579 leaf samples (18 $\pm$ 15 SD samples per taxon). Of the four species that we did not sample, two (*A. virescens* and *D. kenwoodii*) are considered extinct (Carr 1985; Wood 2015) and two (*D. carrii* and *D. hanaulaensis*) are only recently delimited from within *D. linearis* (Baldwin & Friar 2010). We collected leaf samples from field populations on Hawai'i, Maui and Kaua'i (n = 421), from glasshouse populations maintained by the National Park Service on Maui or the National Tropical Botanical Garden on Kaua'i (n = 65), or from dried material excised from collections in the herbarium of the National Tropical Botanical Garden (n = 93).

We focused on assessing the biological significance of variation across taxa at the macroevolutionary scale rather than within taxa. We typically sampled one population per taxon, mainly because most taxa in the silversword alliance are now either endangered, threatened, vulnerable, or rare, reflecting the severity of the threats posed by alien species in Hawai'i (Purugganan & Robichaux, 2005). Though we were not able to consistently assess within-taxon (i.e. among-population) variation or phenotypic plasticity in leaf functional traits, earlier work indicates that neither is large compared to between-taxon variation in the silversword alliance. For example, a comprehensive analysis of variance partitioning in leaf size across hierarchies of population structure in recently derived, parapatric (and currently less imperilled) *Dubautia* taxa demonstrated that more than 90% of the partitioning occurs between rather than within taxa (Lawton-Rauh, Robichaux & Purugganan 2007), even in the face of significant historical and contemporary gene flow (Remington & Robichaux 2007). Additionally, an assessment of the degree of phenotypic variation (or plasticity) in leaf functional traits related to turgor maintenance capacity and thus leaf water balance across contrasting growth regimes and seasons showed such variation to be low within *Dubautia* taxa, especially compared to the large differences in trait values between taxa (Robichaux 1984; Robichaux & Canfield 1985).

Table 1. Summary of collections of silversword alliance taxa used in this study

Name	Code	Range	Habit	Habitat	Provenance	Samples	In tree
Argyroxiphium caliginis	ACLG	Ma	Rosette	b	Herbarium	6	x
Argyroxiphium grayanum	AGRY	Ma	Rosette	b, w	Greenhouse	50	x
Argyroxiphium kauense Kau form	AKNSK	Ha	Rosette	w	Field	50	x
Argyroxiphium kauense Waiakea form	AKNSW	Ha	Rosette	b	Field	50	
Argyroxiphium sandwicense subsp. *sandwicense*	ASNDS	Ha	Rosette	d, c	Field	35	x
Dubautia arborea	DRBR	Ha	Tree	d	Field	35	x
Dubautia ciliolata subsp. *glutinosa*	DCLLG	Ha	Shrub	d, c	Field	35	x
Dubautia herbstobatae	DHRB	Oa	Shrub	d	Greenhouse	3	x
Dubautia imbricata subsp. *imbricata*	DMBRI	Ka	Shrub	w	Herbarium	3	x
Dubautia kalalauensis	DKLL	Ka	Shrub	w	Greenhouse	3	
Dubautia knudsenii subsp. *filiformis*	DKNDF	Ka	Shrub	w	Herbarium	9	x
Dubautia knudsenii subsp. *knudsenii*	DKNDK	Ka	Tree	w	Field	25	x
Dubautia knudsenii subsp. *nagatae*	DKNDN	Ka	Shrub	w	Field	4	x
Dubautia laevigata	DLVG	Ka	Shrub	w	Herbarium	3	x
Dubautia latifolia	DLTF	Ka	Liana	w	Herbarium	6	x
Dubautia laxa subsp. *hirsuta*	DLX	La, Oa, Ka	Shrub	b	Field	18	x
Dubautia linearis subsp. *hillebrandii*	DLNRH	Ha	Shrub	d, c	Field	50	x
Dubautia menziesii	DMNZ	Ma	Shrub	d, c	Field	30	x
Dubautia microcephala	DMCR	Ka	Shrub	w	Herbarium	6	x
Dubautia paleata	DPLT	Ka	Shrub	b, w	Field	20	x
Dubautia pauciflorula	DPCF	Ka	Shrub	w	Herbarium	7	x
Dubautia plantaginea subsp. *humilis*	DPLNH	Ma	Shrub	w	Herbarium	6	x
Dubautia platyphylla	DPLT	Ma	Shrub	d	Field	25	x
Dubautia raillardioides	DRLL	Ka	Shrub	w	Field	20	x
Dubautia reticulata	DRTC	Ma	Tree	w	Field	5	x
Dubautia scabra subsp. *leiophylla*	DSCBL	Ha, Ma, Mo, La	Shrub	w	Herbarium	12	x
Dubautia sherffiana	DSHR	Oa	Shrub	w	Herbarium	9	x
Dubautia syndetica	DSYN	Ka	Shrub	w	Herbarium	9	
Dubautia waialealae	DWLL	Ka	Cushion	b	Herbarium	8	
Dubautia waianapanapaensis	DWNP	Ma	Shrub	w	Herbarium	9	
Wilkesia gymnoxiphium	WGYM	Ka	Rosette	d	Field	25	x
Wilkesia hobdyi	WHBD	Ka	Rosette	d	Greenhouse	3	x

Range abbreviations denote the major Hawaiian Islands: Ha, Hawai'i; Ma, Maui; Mo, Moloka'i; La, Lana'i; Oa, O'ahu; Ka, Kaua'i. Habitat abbreviations: b, bog; c, cinder and lava; d, dry shrubland and woodland; w, wet shrubland and forest. Taxa flagged as 'in tree' are included in the molecular phylogenies.

LEAF FUNCTIONAL TRAIT DATA

We measured leaf area (LA) for mature leaves using non-destructive methods. For shorter leaves, we traced the outline of the leaf onto paper and later digitized these tracings. Otherwise, for long leaves without significant curvature, we estimated LA by definite integration using the trapezoid rule, measuring leaf length and leaf width at five evenly spaced intervals. With herbarium material, a key source for the more imperilled taxa, LA was measured for dried specimens, recognizing that this produces a small potential bias due to shrinkage (Blonder *et al.* 2012a). Leaf elongation ratio (LER) was calculated as leaf length divided by leaf maximum width. We measured leaf thickness (d) on fresh field-collected leaves by averaging three measurements at evenly spaced points along the lamina. We did not measure d for compressed, dried herbarium specimens.

For measurements of dry mass and elemental compositions/ratios (N_m, C_m, P_m, $\delta^{13}C$ and $\delta^{15}N$), we collected mature leaves, taking a whole leaf (including petiole) where possible. Otherwise, we cut a 2×2 cm^2 section from the leaf lamina (e.g. from herbarium specimens). We dried each sample first in a chemical desiccant (anhydrous calcium sulphate) and later at 60°C for several days in a large oven. We measured dry mass of each sample using a digital balance. For each taxon, we measured N_m, C_m, P_m, $\delta^{13}C$ and $\delta^{15}N$ by pooling dried and ground material from the leaf samples ($n = 4.6 \pm 2.3$ SD leaves per taxon). N_m, C_m, $\delta^{13}C$ and $\delta^{15}N$ were measured in the Environmental Isotope Laboratory at the University of Arizona with a continuous-flow gas-ratio mass spectrometer (Finnigan Delta PlusXL) coupled to an elemental analyser. Samples of 1.0 ± 0.2 mg were combusted in the elemental analyser (Costech). Standardization was based on acetanilide for elemental concentrations, NBS-22 and USGS-24 for $\delta^{13}C$ and IAEA-N-1 and IAEA-N-2 for $\delta^{15}N$. Precision was at least ± 0.1 for $\delta^{13}C$ and ± 0.2 for $\delta^{15}N$ (1s) based on repeated internal standards. P_m was measured in the Enquist laboratory at the University of Arizona via colorimetry with a spectrophotometer (ThermoScientific Genesys20, Waltham, MA, USA) after persulphate oxidation followed by the acid molybdate technique.

We obtained leaf venation network images with synchrotron X-ray absorption-contrast imaging at the Advanced Photon Source at Argonne National Laboratory (Argonne, IL, USA) following the protocol described in Blonder *et al.* (2012b). Final image resolution was 3.56 μm pixel^{-1} (281 pixels mm^{-1}). This method has been shown to accurately image the minor venation networks of leaves with a wide range of morphologies (Blonder *et al.* 2012b). Additionally, the images were qualitatively similar to, though more detailed than, those previously reported based on chemical methods for a few silversword alliance taxa (Carlquist 1959). To estimate vein density (VD) and vein elongation index (VEI), we first hand-traced each leaf venation network image. We next inferred the skeleton of each image and segmented each areole (region of lamina enclosed by venation) using

MATLAB's Image Analysis Toolkit. We estimated VD as the length of all veins in the image divided by the image area. We estimated VEI as the mean of the ratio of major to minor axes of an ellipse fitted to each areole.

CLIMATE DATA

We estimated the climate niche position for each taxon by integrating occurrence records and gridded climate data. For each leaf we collected in the field, we recorded the latitude and longitude of the locality using a GPS. For each leaf we sampled from a herbarium, we obtained latitude and longitude by geo-referencing the specimen's collection locality notes. We did not record latitude and longitude for the small set of leaves sampled from glasshouses. We then transformed each location to a climate value using gridded data for T_{min} [PRISM 800 m resolution, 1971–2000 average (PRISM, 2006)], mean annual precipitation (MAP; mm) [Rainfall Atlas of Hawai'i 250 m resolution, 1978–2007 means (Giambelluca *et al.* 2013)] and aridity index (AI) [CGIAR-CSI Global-Aridity and Global-PET Database, 1000 m resolution, 1950–2000 means (Zomer *et al.* 2008)]. We estimated the climate niche position for each taxon based on the means of the respective T_{min}, MAP and AI values across all leaves sampled. The PRISM and CGIAR data bases, with their ~1 km resolutions, may introduce some error because the high topographic heterogeneity in Hawai'i can lead to climate heterogeneity not captured by the model. We expect this error to be relatively constant across our analyses. Although more detailed data are available for some locations in Hawai'i, such as on Haleakalā volcano (Longman *et al.* 2015), we opted to use the PRISM and CGIAR data bases because their complete spatial coverage of divergent habitats likely outweighed any error in values.

PHYLOGENETIC DATA

To analyse trait–trait and trait–climate relationships in a phylogenetic context, we obtained a set of 30 000 ultrametric trees for 27 taxa in the silversword alliance from Bayesian phylogenetic analyses of nuclear ribosomal DNA ITS sequences (Baldwin & Sanderson 1998). Our focus on ITS sequences to the exclusion of chloroplast DNA data was based largely on the high level of phylogenetic congruence between ITS trees and cytogenetic data (i.e. nuclear genomic arrangements) for the silversword alliance (Carr & Kyhos 1986), in contrast to strong phylogenetic incongruence between chloroplast DNA data and both nuclear data sets, evidently as a result of extensive chloroplast capture (Baldwin 2003). In addition, ITS sequences are unusually well suited for generating the ultrametric trees because of approximately clock-like ITS evolution during diversification of the silversword alliance (Baldwin & Sanderson 1998). Four taxa for which we obtained leaf functional trait data were not encompassed by the ITS data set (*D. kalalauensis, D. syndetica, D. waialealae* and *D. waianapanapaensis*).

The ITS sequence alignment of Baldwin & Sanderson (1998) for taxa in common with the present study compared favourably using the similarity criterion of Simmons (2004) to a highly similar alignment using MAFFT v. 7.017 (Katoh & Standley 2013) and was used here (available on TreeBASE at http://purl.org/phylo/treebase/phylows/study/TB2:S17478). We conducted the phylogenetic analyses in BEAST v1.7.5 (Drummond & Rambaut 2007) using a partitioned model of sequence evolution (TrNef+G for ITS-1 and ITS-2; TrNef+I for the 5.8S subunit) identified as best using the Bayesian Information Criterion (BIC) in PartitionFinder (Lanfear *et al.* 2012). Three North American perennial tarweeds (*Anisocarpus madioides*, *A. scabridus* and *Carlquistia muirii*) in the 'Madia' lineage (Baldwin 2003) served as the out-group, with the in-group constrained to be monophyletic. A log-normal relaxed clock (uncorrelated) model of evolutionary rates across lineages was chosen, although only minor rate heterogeneity was detected using TRACER 1.5 (Rambaut & Drummond 2009) based on values well under 1.0 for the coefficient of variation parameter. The distance from root to tips in the ultrametric trees was scaled to 1.0. A Yule process model of speciation was used, based on results of model tests for the silversword alliance by Baldwin & Sanderson (1998).

Four independent Markov chain Monte Carlo (MCMC) analyses of 10 million generations each were run to completion, with sampling of one tree from the posterior distribution every 1000 generations. A 25% burn-in for each chain was determined to be conservative using TRACER v1.5 to examine stationarity of tree likelihoods and convergence of the posterior distribution based on effective sample size scores (> 500 for all parameters in the final distribution) and the graphical output for each run, using LOGCOMBINER v1.7.5 in the BEAST package. The 95% majority rule consensus tree of sampled trees in the posterior distribution also was compared to the maximum likelihood (ML) tree resolved using RAXML-HPC2 (Stamatakis 2006), as implemented on XSEDE by the CIPRES Science Gateway (http://www.phylo.org/sub_sections/portal/; using default settings except for implementing separate partitions for ITS-1+ITS2 and the 5.8S gene) and found to be of nearly identical topology, with > 70% ML rapid bootstrap support for the same sublineages that were well-supported in the Bayesian analysis.

STATISTICAL ANALYSES

We conducted all analyses in R version 3.1.2 (http://www.r-project.org). ANOVAS were computed using the 'stats' package with Type II sums of squares. We evaluated all variables for normality with quantile–quantile plots, then applied a $\log_{10}$ transformation to VD, VEI, LMA, *d*, LA, LER, C_m, N_m, P_m, T_{min}, AI and MAP.

We assessed pairwise correlations for trait–trait and trait–climate relationships with phylogenetic regression ['ape' (Paradis, Claude & Strimmer 2004) and 'phyloch' packages (Heibl 2013)]. We used generalized least squares (GLS) regression on taxon-mean data. We evaluated white-noise, random-walk and Ornstein–Uhlenbeck (frictional random-walk) evolutionary models as explanatory models, following guidance for examining phylogenetic niche conservatism (Wiens *et al.* 2010; Pyron *et al.* 2015). All analyses omitted data for missing leaf functional trait or climate values or missing taxa. We repeated analyses for a regular sample of 10 000 trees from the posterior distribution of phylogenetic trees and for each evolutionary model. Specifically, we used the 'gls' function with the 'correlation' argument set to either NULL (white-noise), corBrownian (1, tree) (random-walk), or corMartins (1, tree) (Ornstein-Uhlenbeck), where tree refers to a phylogenetic tree sampled from the posterior distribution. We then assessed the fraction of times each GLS model obtained the lowest Akaike information criterion (AIC) score, the distribution of coefficients, and the fraction of times the coefficient *P*-value was significant (at $\alpha = 0.05$). We did not correct *P*-values to account for multiple comparisons because our primary goal was to assess the evolutionary model fit for the widest set of possibly valid pairwise relationships; that is to perform the analysis with the highest power possible. The causal analysis described below is aimed at rejecting hypotheses for individual pairwise relationships.

We assessed the causal structure of leaf venation network theory with structural equation modelling ['lavaan' package (Rosseel 2012)]

using $\log_{10}$-transformed taxon-mean data. We used 'cause' to mean that A caused B if variation in A was associated with linearly correlated variation in B, but that variation in B was not necessarily associated with linearly correlated variation in A (Shipley 2000). We determined if the model was consistent with observed data by computing a lack-of-fit chi-square statistic using maximum likelihood estimation. If this p-value is large, then the model cannot be rejected given the data.

Results

EMPIRICAL PATTERNS OF FUNCTIONAL INTEGRATION

There was very high variation both in leaf functional traits and in climate niche parameters across the silversword alliance (Figs 1 and 2). The ranges across leaf specimens for many of the leaf functional traits (listed in Fig. 2) spanned a substantial fraction of the respective global angiosperm ranges. [e.g. 14–1500 g m^{-2} for LMA (Wright *et al.* 2004), 0.2–6.4% for N_m (Wright *et al.* 2004), 0.2–0.7 mm 95% quantile range for d and 1–25 mm^{-1} for VD (Brodribb, Feild & Jordan 2007; Kattge *et al.* 2011)]. Values of VEI are not widely reported, so there is no global comparison for the large range detected across the silversword alliance. Approximate ranges for other traits can be found in Kattge *et al.* (2011).

Leaf functional traits showed strong integration (covariation) across silversword alliance taxa. A negative correlation existed between LMA and N_m ($r^2 = 0.28$, $P < 0.002$) that recapitulated what is seen in the global leaf economics spectrum (Wright *et al.* 2004). Assessing all leaf functional traits and climate niche parameters together using $\log_{10}$-transformed values, principal components analysis showed 51% of the variation explained by the first two axes (Fig. S1, Supporting Information). The first axis was dominated by T_{min}, VD, LMA and d; the second by MAP and VEI.

MACROEVOLUTIONARY MODELS OF FUNCTIONAL INTEGRATION

Fifty-four of the $15 \times 14 = 210$ pairwise trait–trait and trait–climate relationships were significant more than 90% of the time under the lowest-AIC evolutionary model (Fig. 3). Forty-three (80%) of the relationships were best explained by a white-noise evolutionary model. Eleven (20%) were best explained by an Ornstein–Uhlenbeck evolutionary model. No relationships (0%) were best explained by a random-walk evolutionary model. In particular, several key predicted metrics of functional integration were best explained by a white-noise evolutionary model, including the leaf economics spectrum relationship between X = LMA and Y = N_m ($P < 0.05$ in 100% of trees; AIC lowest for white-noise in 67% of trees) and the relationships between X = VD and each of Y = LMA, d and T_{min} (in every case, $P < 0.05$ in 100% of trees; AIC lowest for white-noise in $\geq$ 64% of trees). However, neither the predicted relationship between VD and N_m nor the predicted relationships between VEI and any of T_{min}, MAP, or AI were significant.

TESTS OF THEORY

The combined trait-trait and trait-climate predictions of leaf venation network theory were translated into a structural equation model (Fig. 4). In this model, T_{min} statistically caused variation in VD, which in turn statistically caused variation in LMA, d and N_m. Other unresolved covariances between functional traits were also permitted. This causal model could not be rejected by the data (lack-of-fit $P = 0.24$, $\chi^2 = 4.2$, d.f. = 3). In the model, the paths between VD and each of T_{min}, LMA and d were of the correct sign and were significant (all $P < 0.02$), whereas the path between VD and N_m was not significant ($P = 0.08$), consistent with the results of the macroevolutionary analysis above. This model also indicated that there were additional significant covariances between LMA and d and between N_m and each of LMA and d. The results indicated that the model was consistent with the data, but that the data were not sufficient to resolve the directionality of all paths. Other unconsidered models could also be consistent with the data, so this test indicated that the leaf venation network model was *one*, but not necessarily *the only*, viable explanation for the data.

Other traits, such as growth habit, LER and leaf pubescence, appeared to further modulate this functional integration. LMA, d and N_m, for example, each varied significantly with growth habit (ANOVA; all $P < 0.05$). Additionally, both LMA and d were positively correlated with LER and leaf pubescence (sparse to dense), and VD was negatively correlated with leaf pubescence (Fig. 3).

Discussion

Leaf functional traits thus vary across the silversword alliance almost as much as they do across all other angiosperms globally, reflecting the very wide range of climate niches inhabited by the Hawaiian taxa. This diversification in leaf functional traits has occurred within a timeframe of only ca. 4–6 My (Baldwin & Sanderson 1998), further confirming very rapid trait evolution in the silversword alliance compared to other plant lineages (Ackerly 2009), including other diverse Hawaiian lineages [e.g. lobeliads (Givnish, Montgomery & Goldstein 2004) and plantains (Sporck & Sack 2009)].

Most of the significant trait–trait and trait–climate relationships in the silversword alliance, including several key predicted metrics of functional integration, are best explained via our model selection procedure by a white-noise evolutionary model. This result is unlikely to be driven by either phylogenetic uncertainty, given that the majority of sublineages were well resolved by this analysis and are highly congruent with cytogenetic data (i.e. nuclear genomic arrangements) (Carr & Kyhos 1986; Baldwin 2003), or trait uncertainty, given our near-complete sampling of species in the lineage. Instead, this result is more consistent with rapid diversification of taxa into novel environments and a limited importance for phylogenetic niche conservatism (Wiens *et al.* 2010). This inference at the macroevolutionary scale complements a key inference at the microevolutionary scale deriving from molecular population

Variable	Abbreviation	Units	Min	Max
VEI	Vein elongation index	–	1.9	38.5
VD	Vein density	mm^{-1}	0.54	9.1
LER	Leaf elongation ratio	–	1.9	53.3
LA	Leaf area	cm^2	0.11	84.9
d	Leaf thickness	mm	0.3	3.3
LMA	Leaf mass per area ratio	$g\ m^{-2}$	19.7	620.4
$\delta^{15}N$	Nitrogen−15 isotope shift	mil	−7.2	3.3
$\delta^{13}C$	Carbon−13 isotope shift	mil	−31.5	−25.8
P_m	Phosphorus content	%	0.029	0.38
N_m	Nitrogen content	%	0.9	2.6
C_m	Carbon content	%	37.5	44.7
AI	Aridity index	–	0.64	5.0
MAP	Mean annual precipitation	$mm\ yr^{-1}$	532.3	9809.8
T_{min}	Minimum annual temperature	°C	2.8	17.5
Pubescence	Pubescence	–		
Habitat	Habitat	–		
Habit	Habit	–		

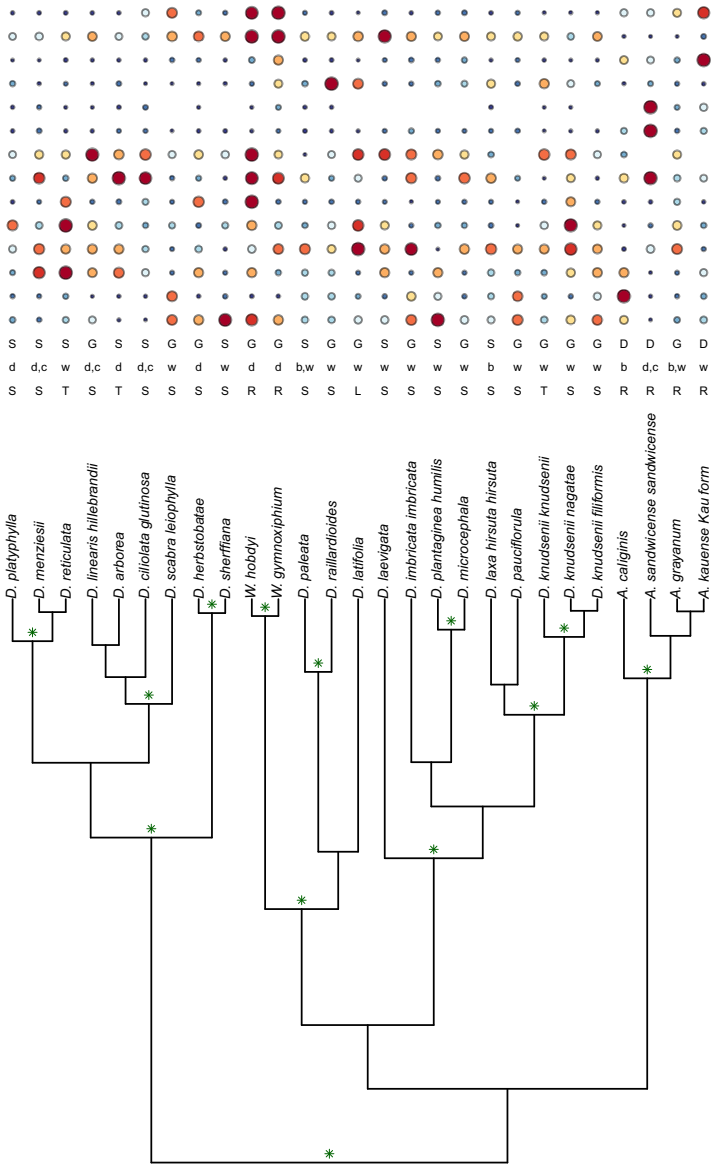

Fig. 2. Evolution of leaf functional traits and climate niche parameters in the silversword alliance based on an ultrametric maximum clade credibility tree. Posterior support values > 0.95 are indicated with green asterisks on internal nodes. Symbol colour and size indicate taxon-mean value; smaller and bluer symbols indicate lower values, whereas larger and redder symbols indicate higher values. The table indicates leaf-level ranges for each trait or parameter. Habit abbreviations are: R, rosette shrub; S, shrub; T, tree; L, liana. Habitat abbreviations are: b, bog; c, cinder and lava; d, dry shrubland and woodland; w, wet shrubland and forest (after Robichaux *et al.* 1990). Pubescence abbreviations are: G, glabrous; S, sparsely pubescent; D, densely pubescent.

genetic analyses of recently derived, parapatric *Dubautia* taxa (Lawton-Rauh, Robichaux & Purugganan 2007; Remington & Robichaux 2007). Specifically, diversifying selection in contrasting ecological settings, especially with respect to moisture availability, has been sufficiently strong (i) to drive substantial quantitative divergence in key vegetative traits (e.g. leaf size, terminal shoot internode length and plant height) and reproductive traits (e.g. number of flowers/capitulum and number of capitula/capitulescence (Lawton-Rauh, Robichaux & Purugganan 2007)) and (ii) to maintain the divergence in the face of significant historical and contemporary gene flow detected at the genome-wide level (Remington & Robichaux 2007). In cases where diversifying selection maintains such large interspecific phenotypic differences in the face of significant gene flow, the number of genetic loci responsible for the differences is expected to be small (Remington & Robichaux 2007).

The functional integration (strong covariation) of leaf traits documented across species in the global leaf economics spectrum (Wright *et al.* 2004) appears to also be evident in the silversword alliance via the observed correlation between LMA and N_m, suggesting that selection is important in driving patterns at multiple scales (Donovan *et al.* 2011). In support of this conjecture, genetic work in *Arabidopsis thaliana*

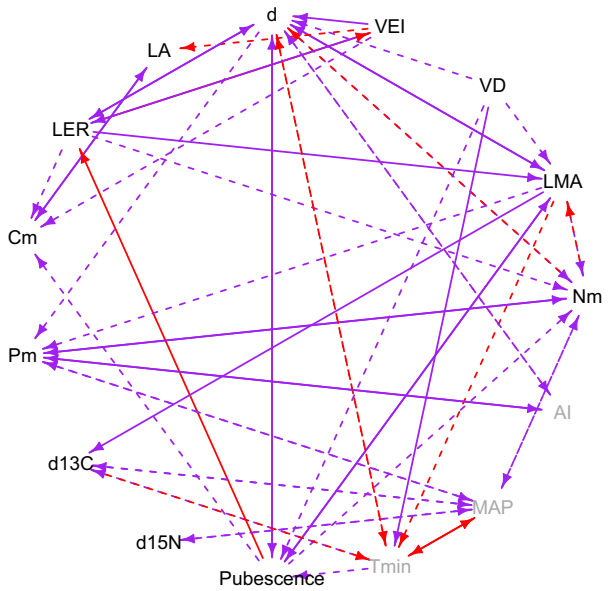

Fig. 3. Phylogenetic correlation network for ordered leaf functional traits and climate niche parameters in the silversword alliance. An arrow from X to Y indicates that X predicts Y, such that a GLS regression for Y~X was significant ($\alpha < 0.05$) in more than 90% of trees for the evolutionary model that obtained the lowest-AIC score. Line colour indicates correlation structure: purple, white-noise evolutionary model; red, Ornstein–Uhlenbeck evolutionary model. No variable pair was best fit by a random-walk evolutionary model. Line type indicates sign: solid, positive; dashed, negative. Label colour indicates variable type: grey if a climate parameter, black if not. Note that some relationships Y~X are best fit by different models than are X~Y, leading to segments with multicoloured heads. Variable abbreviations are defined in Fig. 2.

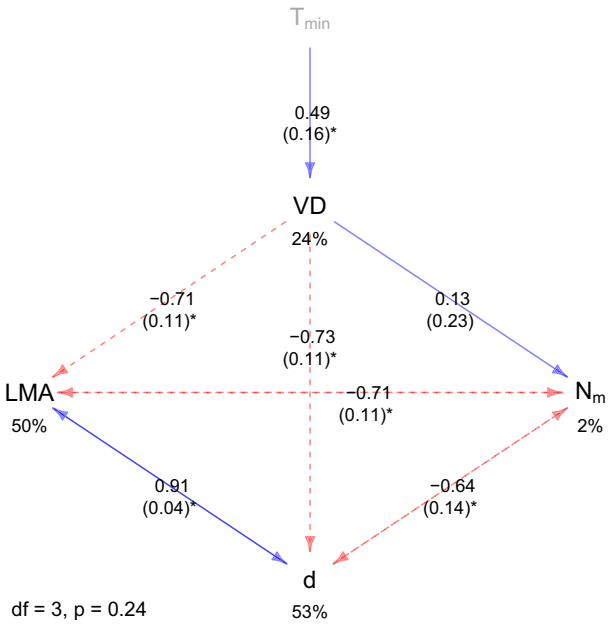

Fig. 4. A structural equation model based on leaf venation network theory for the silversword alliance. The diagram shows the unified trait-trait and trait-climate predictions of leaf venation network theory. Arrows indicate the proposed causal relationships between variables; double arrows indicate unresolved covariances. Labels on arrows indicate standardized path coefficients, with standard errors in parentheses and an asterisk drawn if significant at the $\alpha < 0.05$ level. Paths are drawn with solid blue lines if positive and dashed red lines if negative. Values under dependent variables indicate R^2 values. The independent climate variable is shown in grey. The overall model degrees of freedom and lack-of-fit *P*-value are shown in the lower left corner. Variable abbreviations are defined in Fig. 2.

(Vasseur *et al.* 2012; Blonder *et al.* 2015) has demonstrated that variation in a small set of genetic loci may consistently underlie many leaf economics trait relationships.

Several key trait-trait and trait-climate predictions of leaf venation network theory are found in the silversword alliance, and the overall causal structure of the theory is not rejected by the data. Further, our macroevolutionary analyses suggest that adaptive shifts in these traits have occurred across taxa without a strong effect of phylogenetic niche conservatism. Together, these results are consistent with the optimization assumptions of the theory. However, it is clear that some individual relationships (e.g. between VD and N_m) are weaker than predicted by the theory or are entirely absent. Recent discussions of the theory (Sack *et al.* 2013; Blonder *et al.* 2014) have suggested that its current causal structure may be incomplete, such that the inclusion of major veins or of variation in tissue mass density may be necessary to generate more accurate predictions.

In the silversword alliance, this functional integration appears to be further modulated by other traits such as growth habit, LER and leaf pubescence. This result suggests a macroevolutionary outcome in which more than one strategy arises in response to a given set of environmental challenges (Robichaux *et al.* 1990). Such an outcome is illustrated in striking fashion by *A. sandwicense* subsp. *sandwicense* and *D. ciliolata* subsp. *glutinosa*, two taxa that grow sympatrically throughout dry shrubland habitats at high elevations on Mauna Kea volcano. The former taxon is a rosette shrub with long, densely pubescent leaves of medium LER and low VD, whereas the latter taxon is a diffusely branched shrub with very short, sparsely pubescent leaves of low LER and medium VD (Fig. 2) (Carr 1985).

The significance of leaf venation network reticulation remains elusive. Despite the large range in VEI detected across the silversword alliance, there is no support for the hypothesized relationships between VEI and climate. VEI is positively correlated with LER in the silversword alliance (Fig. 3), suggesting that the developmental processes governing vein areole elongation may be linked to those governing leaf elongation and thus leaf shape (Nicotra *et al.* 2011).

Our results thus highlight the importance of functional diversification and integration in rapidly evolving plant lineages. For the silversword alliance, our demonstration that leaf functional trait variation (i) spans much of the global angiosperm range, (ii) is best explained by a white-noise evolutionary model and (iii) is integrated in ways consistent with both the global leaf economics spectrum and the predictions of leaf venation network theory provides compelling additional support for the view that this rapidly evolving

lineage is indeed 'one of the most remarkable examples of adaptive radiation in plants' (Raven, Evert & Eichhorn 2013).

Acknowledgements

Research permits and site access were coordinated with the U.S. Fish and Wildlife Service, Hawai'i Department of Land and Natural Resources, Nature Conservancy, National Tropical Botanical Garden, Kaua'i State Parks, Haleakalā National Park, Hawai'i Volcanoes National Park and Department of Defense Pōhakuloa Training Area. Emma Wollman co-led fieldwork, designed and built sample holders for X-ray work and helped with imaging. Bryan Helm also helped with X-ray imaging. Vanessa Buzzard helped with laboratory analyses. John Lacson, Lindsey Parker, Nathan May and Courtney Magness assisted with image analysis. Margaret Evans provided comments on early drafts of the manuscript.

BWB was supported by the National Geographic Young Explorers Programme, Sigma Xi and an NSF Pre-doctoral Fellowship. BGB was supported by the McBryde Endowment of the National Tropical Botanical Garden and NSF grant DEB-9458237. BJE was supported by an NSF ATB Award. RHR was supported by U.S. Fish and Wildlife Service Awards. Use of the Advanced Photon Source was supported by the Argonne National Laboratory and U.S. Department of Energy.

Data accessibility

Trait data: The data sets supporting this article have been uploaded as part of the Supporting Information. Data have also been submitted to the TRY data base.(https://www.try-db.org/TryWeb/Home.php). Venation network images are available at the Cleared Leaves Database (http://clearedleavesdb.org/content/hawaiian-silversword-alliance).

DNA sequence alignment and tree data: The phylogenetic trees supporting this article have been uploaded as part of the Supporting Information. Trees and sequence data are available from TreeBASE at http://purl.org/phylo/treebase/phylows/study/TB2:S17478.

References

Ackerly, D. (2009) Conservatism and diversification of plant functional traits: evolutionary rates versus phylogenetic signal. *Proceedings of the National Academy of Sciences of the United States of America*, **106**, 19699–19706.

Baldwin, B. (2003) A phylogenetic perspective on the origin and evolution of the Madiinae. *Tarweeds & Silverswords: Evolution of the Madiinae (Asteraceae)* (eds S. Carlquist, B. Baldwin & G. Carr), pp. 193–228. Missouri Botanical Garden, St. Louis, MO, USA.

Baldwin, B.G. & Friar, E.A. (2010) *Dubautia carrii* and *D. hanaulaensis*, new species of the Hawaiian silversword alliance (Compositae, Madlinae) from Molokai and Maui. *Novon*, **20**, 1–8.

Baldwin, B.G. & Sanderson, M.J. (1998) Age and rate of diversification of the Hawaiian silversword alliance (Compositae). *Proceedings of the National Academy of Sciences of the United States of America*, **95**, 9402–9406.

Barrier, M., Baldwin, B., Robichaux, R. & Purugganan, M.D. (1999) Interspecific hybrid ancestry of a plant adaptive radiation: allopolyploidy of the Hawaiian silversword alliance (Asteraceae) inferred from floral homeotic gene duplications. *Molecular Biology and Evolution*, **16**, 1105–1113.

Blonder, B. & Enquist, B. (2014) Inferring climate from angiosperm leaf venation network geometry. *New Phytologist*, **204**, 116–126.

Blonder, B., Violle, C. & Enquist, B. (2013) Assessing the causes and scales of the leaf economics spectrum using venation networks in *Populus tremuloides*. *Journal of Ecology*, **101**, 981–989.

Blonder, B., Violle, C., Bentley, L.P. & Enquist, B.J. (2011) Venation networks and the origin of the leaf economics spectrum. *Ecology Letters*, **14**, 91–100.

Blonder, B., Buzzard, V., Simova, I., Sloat, L., Boyle, B., Lipson, R. *et al.* (2012a) The leaf-area shrinkage effect can bias paleoclimate and ecology research. *American Journal of Botany*, **99**, 1756–1763.

Blonder, B., Carlo, F., Moore, J., Rivers, M. & Enquist, B.J. (2012b) X-ray imaging of leaf venation networks. *New Phytologist*, **196**, 1274–1282.

Blonder, B., Violle, C., Patrick Bentley, L. & Enquist, B. (2014) Inclusion of vein traits improves predictive power for the leaf economic spectrum: a response to Sack et al. (2013). *Journal of Experimental Botany*, **65**, 5109–5114.

Blonder, B., Vasseur, F., Violle, C., Shipley, B., Enquist, B.J. & Vile, D. (2015) Testing models for the leaf economics spectrum with leaf and whole-plant traits in *Arabidopsis thaliana*. *AoB Plants*, **7**, doi: 10.1093/aobpla/plv049.

Boyce, C.K., Brodribb, T.J., Feild, T.S. & Zwieniecki, M.A. (2009) Angiosperm leaf vein evolution was physiologically and environmentally transformative. *Proceedings of the Royal Society B: Biological Sciences*, **276**, 1771–1776.

Brodribb, T.J., Feild, T.S. & Jordan, G.J. (2007) Leaf maximum photosynthetic rate and venation are linked by hydraulics. *Plant Physiology*, **144**, 1890–1898.

Brodribb, T.J., Feild, T.S. & Sack, L. (2010) Viewing leaf structure and evolution from a hydraulic perspective. *Functional Plant Biology*, **37**, 488–498.

Brodribb, T.J., Jordan, G.J. & Carpenter, R.J. (2013) Unified changes in cell size permit coordinated leaf evolution. *New Phytologist*, **199**, 559–570.

Carlquist, S. (1959) Vegetative anatomy of *Dubautia, Argyroxiphium* and *Wilkesia* (Compositae). *Pacific Science*, **13**, 195–210.

Carr, G. (1985) Monograph of the Hawaiian Madiinae (Asteraceae): *Argyroxiphium, Dubautia*, and *Wilkesia*. *Allertonia*, **4**, 1–123.

Carr, G. & Kyhos, D. (1986) Adaptive radiation in the Hawaiian silversword alliance (Compositae–Madiinae). II. Cytogenetics of artificial and natural hybrids. *Evolution*, **40**, 959–976.

Crisp, M.D. & Cook, L.G. (2012) Phylogenetic niche conservatism: what are the underlying evolutionary and ecological causes? *New Phytologist*, **196**, 681–694.

Donovan, L.A., Maherali, H., Caruso, C.M., Huber, H. & de Kroon, H. (2011) The evolution of the worldwide leaf economics spectrum. *Trends in Ecology & Evolution*, **26**, 88–95.

Drummond, A.J. & Rambaut, A. (2007) BEAST: Bayesian evolutionary analysis by sampling trees. *BMC Evolutionary Biology*, **7**, 214.

Ellis, B., Daly, D., Hickey, L., Johnson, K., Mitchell, J., Wilf, P. & Wing, S. (2009) *Manual of Leaf Architecture*. Cornell University Press, Ithaca, NY, USA.

Giambelluca, T.W., Chen, Q., Frazier, A.G., Price, J.P., Chen, Y.-L., Chu, P.-S., Eischeid, J.K. & Delparte, D.M. (2013) Online rainfall atlas of Hawai'i. *Bulletin of the American Meteorological Society*, **94**, 313–316.

Givnish, T.J., Montgomery, R.A. & Goldstein, G. (2004) Adaptive radiation of photosynthetic physiology in the Hawaiian lobeliads: light regimes, static light responses, and whole-plant compensation points. *American Journal of Botany*, **91**, 228–246.

Givnish, T.J., Pires, J.C., Graham, S.W., McPherson, M.A., Prince, L.M., Patterson, T.B., Rai, H.S., Roalson, E.H., Evans, T.M. & Hahn, W.J. (2005) Repeated evolution of net venation and fleshy fruits among monocots in shaded habitats confirms *a priori* predictions: evidence from an *ndhF* phylogeny. *Proceedings of the Royal Society B: Biological Sciences*, **272**, 1481–1490.

Heibl, C. (2013) PHYLOCH: R language tree plotting tools and interfaces to diverse phylogenetic software packages available at: http://www.christophheibl.de/Rpackages.html.

Katifori, E., Szöllősi, G.J. & Magnasco, M.O. (2010) Damage and fluctuations induce loops in optimal transport networks. *Physical Review Letters*, **104**, 048704.

Katoh, K. & Standley, D.M. (2013) MAFFT multiple sequence alignment software version 7: improvements in performance and usability. *Molecular Biology and Evolution*, **30**, 772–780.

Kattge, J., Díaz, S., Lavorel, S., Prentice, I.C., Leadley, P., Bönisch, G. *et al.* (2011) TRY – a global database of plant traits. *Global Change Biology*, **17**, 2905–2935.

Lanfear, R., Calcott, B., Ho, S.Y.W. & Guindon., S. (2012) PartitionFinder: combined selection of partitioning schemes and substitution models for phylogenetic analyses. *Molecular Biology and Evolution*, **29**, 1695–1701.

Lawton-Rauh, A., Robichaux, R.H. & Purugganan, M.D. (2007) Diversity and divergence patterns in regulatory genes suggest differential gene flow in recently derived species of the Hawaiian silversword alliance adaptive radiation (Asteraceae). *Molecular Ecology*, **16**, 3995–4013.

Li, L., McCormack, M.L., Ma, C., Kong, D., Zhang, Q., Chen, X., Zeng, H., Niinemets, Ü. & Guo, D. (2015) Leaf economics and hydraulic traits are decoupled in five species-rich tropical-subtropical forests. *Ecology Letters*, **18**, 899–906.

Longman, R., Giambelluca, T.W., Nullet, M. & Loope, L.L. (2015) Technical Report 193: Climatology of Haleakala¯. The Pacific Cooperative Studies Unit, University of Hawaii at Manoa http://manoa.hawaii.edu/hpicesu/techr/193/v193.pdf.

McKown, A., Cochard, H. & Sack, L. (2010) Decoding leaf hydraulics with a spatially explicit model: principles of venation architecture and implications for its evolution. *The American Naturalist*, **175**, 447–460.

Nicotra, A.B., Leigh, A., Boyce, C.K., Jones, C.S., Niklas, K.J., Royer, D.L. & Tsukaya, H. (2011) The evolution and functional significance of leaf shape in the angiosperms. *Functional Plant Biology*, **38**, 535–552.

Niinemets, Ü., Portsmuth, A., Tena, D., Tobias, M., Matesanz, S. & Valladares, F. (2007) Do we underestimate the importance of leaf size in plant

economics? Disproportional scaling of support costs within the spectrum of leaf physiognomy. *Annals of Botany*, **100**, 283–303.
Noblin, X., Mahadevan, L., Coomaraswamy, I.A., Weitz, D.A., Holbrook, N.M. & Zwieniecki, M.A. (2008) Optimal vein density in artificial and real leaves. *Proceedings of the National Academy of Sciences of the United States of America*, **105**, 9140–9144.
Paradis, E., Claude, J. & Strimmer, K. (2004) APE: analyses of phylogenetics and evolution in R language. *Bioinformatics*, **20**, 289–290.
Price, C.A. & Weitz, J.S. (2014) Costs and benefits of reticulate leaf venation. *BMC Plant Biology*, **14**, 234.
PRISM (2006) PRISM Climate Group. Oregon State University http://prism.oregonstate.edu.
Purugganan, M.D. & Robichaux, R.H. (2005) Adaptive radiation and regulatory gene evolution in the Hawaiian silversword alliance (Asteraceae). *Annals of the Missouri Botanical Garden*, **92**, 28–35.
Pyron, R.A., Costa, G.C., Patten, M.A. & Burbrink, F.T. (2015) Phylogenetic niche conservatism and the evolutionary basis of ecological speciation. *Biological Reviews*, **90**, 1248–1262.
Rambaut, A. & Drummond, A.J. (2009) *Tracer* v1.5, avaliable at: http://tree.bio.ed.ac.uk/software/tracer/.
Raven, P.H., Evert, R.F. & Eichhorn, S.E. (2013) *Biology of Plants*. W.H. Freeman, New York, NY, USA.
Remington, D.L. & Robichaux, R.H. (2007) Influences of gene flow on adaptive speciation in the *Dubautia arborea–D. ciliolata* complex. *Molecular Ecology*, **16**, 4014–4027.
Robichaux, R.H. (1984) Variation in the tissue water relations of two sympatric Hawaiian *Dubautia* species and their natural hybrid. *Oecologia*, **65**, 75–81.
Robichaux, R.H. & Canfield, J.E. (1985) Tissue elastic properties of eight Hawaiian *Dubautia* species that differ in habitat and diploid chromosome number. *Oecologia*, **66**, 77–80.
Robichaux, R.H., Carr, G.D., Liebman, M. & Pearcy, R.W. (1990) Adaptive radiation of the Hawaiian silversword alliance (Compositae-Madiinae): ecological, morphological, and physiological diversity. *Annals of the Missouri Botanical Garden*, **77**, 64–72.
Rosseel, Y. (2012) lavaan: an R package for structural equation modeling. *Journal of Statistical Software*, **48**, 1–36.
Sack, L. & Holbrook, N.M. (2006) Leaf hydraulics. *Annual Review of Plant Biology*, **57**, 361–381.
Sack, L. & Scoffoni, C. (2013) Leaf venation: structure, function, development, evolution, ecology and applications in the past, present and future. *New Phytologist*, **198**, 983–1000.
Sack, L., Scoffoni, C., John, G.P., Poorter, H., Mason, C.M., Mendez-Alonzo, R. & Donovan, L.A. (2013) How do leaf veins influence the worldwide leaf economic spectrum? Review and synthesis. *Journal of Experimental Botany*, **64**, 4053–4080.
Shipley, B. (2000) *Cause and Correlation in Biology: A User's Guide to Path Analysis, Structural Equations and Causal Inference*. Cambridge University Press, Cambridge, UK.
Simmons, M.P. (2004) Independence of alignment and tree search. *Molecular Phylogenetics and Evolution*, **31**, 874–879.
Sporck, M.J. & Sack, L. (2009) Leaf trait diversification and design in seven rare taxa of the Hawaiian *Plantago* radiation. *International Journal of Plant Sciences*, **170**, 61–75.
Stamatakis, A. (2006) RAxML-VI-HPC: maximum likelihood-based phylogenetic analyses with thousands of taxa and mixed models. *Bioinformatics*, **22**, 2688–2690.
Stamatakis, A., Hoover, P. & Roguemont, J. (2008) A fast bootstrapping algorithm for the RAxML web-servers. *Systematic Biology*, **57**, 758–771.
Vasseur, F., Violle, C., Enquist, B.J., Granier, C. & Vile, D. (2012) A common genetic basis to the origin of the leaf economics spectrum and metabolic scaling allometry. *Ecology Letters*, **15**, 1149–1157.
Wiens, J.J. (2004) Speciation and ecology revisited: phylogenetic niche conservatism and the origin of species. *Evolution*, **58**, 193–197.
Wiens, J.J., Ackerly, D.D., Allen, A.P., Anacker, B.L., Buckley, L.B., Cornell, H.V. *et al.* (2010) Niche conservatism as an emerging principle in ecology and conservation biology. *Ecology Letters*, **13**, 1310–1324.
Wood, K. (2015) Survey results for eight possibly extinct plant species from Kaua'i, Hawaii. U.S. Fish and Wildlife Service Report F12AC00737.
Wright, I.J., Reich, P.B., Westoby, M., Ackerly, D.D., Baruch, Z., Bongers, F. *et al.* (2004) The worldwide leaf economics spectrum. *Nature*, **428**, 821–827.
Zomer, R., Trabucco, A., Bossio, D. & Verchot, L. (2008) Climate change mitigation: a spatial analysis of global land suitability for clean development mechanism afforestation and reforestation. *Agriculture, Ecosystems & Environment*, **126**, 67–80.

Received 16 May 2015; accepted 19 October 2015
Handling Editor: Jennifer Lau

Supporting Information

Additional Supporting Information may be found in the online version of this article:

Appendix S1. CSV file containing leaf-level measurements.

Appendix S2. Posterior distribution of phylogenetic trees for the silversword alliance.

Figure S1. Biplot of principal components analysis of leaf functional traits and climate niche parameters in the silversword alliance.